PHOTONICS Research

Dark dimer mode excitation and strong coupling with a nanorod dipole

Yixiao Gao,[1,*] Ning Zhou,[1] Zhangxing Shi,[1] Xin Guo,[1] and Limin Tong[1,2,3]

[1]State Key Laboratory of Modern Optical Instrumentation, College of Optical Science and Engineering, Zhejiang University, Hangzhou 310027, China
[2]Collaborative Innovation Center of Extreme Optics, Shanxi University, Taiyuan 030006, China
[3]e-mail: phytong@zju.edu.cn
*Corresponding author: yixiaogao@zju.edu.cn

Received 15 June 2018; revised 23 July 2018; accepted 23 July 2018; posted 24 July 2018 (Doc. ID 335350); published 21 August 2018

We theoretically investigate dark dimer mode excitation and strong coupling with a nanorod dipole. Efficient excitation of a dark mode in a gold (Au) nanorod dimer using an electric dipole can be achieved by an optimal overlap between the dipole moment and dark modal field. By replacing the dipole emitter with an Au nanorod, a plane wave excited dipole mode in the nanorod can be effectively coupled to the dark dimer mode through near-field interaction. At a 10-nm separation of the nanorod and the dimer, plasmonic interaction between dipole-dark modes enters the strong coupling regime with a Rabi-like splitting of 219.2 meV, which is further evidenced by the anticrossing feature and Rabi-like oscillation of electromagnetic energy of the coupled modes. Our results propose an efficient approach to far-field activating dark modes in coupled nanorod dimers and exchanging plasmonic excitations at nanoscale, which may open new opportunities for nanoplasmonic applications such as nanolasers or nanosensors.

OCIS codes: (250.5403) Plasmonics; (230.4555) Coupled resonators; (240.6680) Surface plasmons.

https://doi.org/10.1364/PRJ.6.000887

1. INTRODUCTION

Surface plasmons, collective photon-electron coupled oscillations on the surface of metal nanostructures, offer an attractive method to manipulate light at subdiffractive scale [1]. Metallic nanoparticles support localized surface plasmon resonance (LSPR) with enhanced near field in their vicinity, showing remarkable potential in plasmon laser [2], biosensing [3], and quantum applications [4,5]. The LSPR interaction in coupled metal nanoparticles exhibits similar characteristics as the hybridization of electron wave functions in atomic orbitals; therefore, metal nanoparticles can be referred to as "plasmonic atoms" [6]. In recent years, mimicking classical atomic and molecular phenomena in plasmonic systems has been an important research topic to realize metallic nanostructures with tailored optical properties, for example, plasmonic analog of electromagnetically induced transparency (EIT) in a metasurface for the slow-light effect [7] and Fano resonance in an engineered plasmonic atom for directional light scattering [8] and high-sensitivity molecular sensing [9].

A plasmonic dimer is a pair of closely placed metal nanoparticles, which has been widely studied due to its geometric simplicity and resonance tunability. The bonding hybridization of dipolar resonance in each nanoparticle creates a "hot spot" where the electromagnetic field in the dimer junction is greatly enhanced [10,11]. The hot spot effect in plasmonic dimers has been exploited in boosting optical nonlinearity [12], the spontaneous emission rate of quantum emitters [13], and detection sensitivity towards single-molecule levels [14]. The antibonding interaction of dipolar resonances, on the other hand, results in a hybridized dimer mode with a vanishing dipole moment, which makes it difficult to interact with free-space radiation and thus appears as a dark mode [10,15]. The dark mode feature could also be found in high-order multipolar LSPR in single nanoparticles [16]. The suppressed radiation renders dark modes better able to store electromagnetic energy and is desired in plasmonic applications requiring lower loss [17], such as plasmon lasing [18,19] and plasmon-exciton coupling [20]. In addition, activating these dark modes by near-field excitation can also trigger Fano or EIT-like responses in coupled nanoparticles [21–25].

Strong coupling in plasmonic systems is attracting growing research interest. The spectral splitting feature of strong coupling was observed in either metallic structures such as nanorod dimer lattices [26], plasmonic Fabry–Perot (F-P) cavity coupling with nanorods [27,28], and nanowire arrays [29], or dielectric-metallic hybrid systems such as nanorod-microfiber

coupled cavities [30] and dielectric multilayer F-P cavities coupling to plasmonic disk dimers [31]. One approach to further facilitating strong coupling is lowering the dissipation rate, which could be achieved by employing nanostructures supporting dark modes without radiative decay.

In this paper, we numerically investigate dark dimer mode excitation and plasmonic strong coupling between dipole modes in a single gold (Au) nanorod, and antibonding dark mode in an end-to-end Au nanorod dimer, using the finite-difference time-domain method (Lumerical). We first studied excitation of bright and dark dimer modes using an electric dipole with different locations and dipole moment orientation. Next, utilizing the narrow-linewidth dark-mode resonance in a nanorod dimer, we show that plane-wave excited dipole resonance in a nanorod can be strongly coupled to the dark mode in a nanorod dimer through near-field interaction with the energy exchange rate surpassing the plasmonic decay; the dependence of spectral splitting on coupling distance is investigated and examined by the strong coupling criterion. Finally, we demonstrate the anticrossing behavior of the dipole nanorod mode and dark dimer mode as well as the Rabi-like oscillation of energy exchange between the strongly coupled modes.

2. RESULTS AND DISCUSSIONS

Au nanorods synthesized by low-cost bottom-up methods have the advantages of single crystalline and better morphology uniformity, which are highly desired building blocks for visible to near-infrared nanoplasmonic applications [32]. A single nanorod supports longitudinal plasmonic dipole modes, as depicted in Fig. 1(a). The resonant frequency of the dipole mode is related to the rod length and diameter, which experiences a redshift with increasing rod length or decreasing rod diameter [32]. When two nanorods are brought together in an end-to-end configuration, as shown in Fig. 1(a), the dipole mode starts to hybridize, due to near-field interaction, into new modes in the nanorod dimer, i.e., bonding mode and antibonding mode. The bonding mode possesses a net dipole moment and is able to interact with free-space radiation (i.e., bright mode), while the antibonding mode has a vanishing dipole moment, cannot easily couple with an external electromagnetic wave and is thus the dark dimer mode. Figure 1(b) shows the calculated dependence of resonant wavelengths of the bright and dark modes of a nanorod dimer on the spacing d, with the permittivity of Au taken from Johnson and Christy's data [33]. Here each nanorod is 20 nm in diameter and 95 nm in length. The bright mode has a longer resonant wavelength than the dark. Modal hybridization increases with decreasing d, leading to a larger resonant wavelength difference between the two modes, while both bright and dark resonant wavelengths converge to the dipole resonant wavelength of the single Au nanorod, with d approaching infinity.

Figure 1(c) demonstrates the absorption spectra of the nanorod dimer (spacing 10 nm) under different electric dipole source excitation conditions. The electric dipole with a dipole moment $\boldsymbol{p}$ is placed 20 nm away from the nanorod dimer. The results can be categorized into five cases: (i) when the electric dipole is located at the dimer end and $\boldsymbol{p}$ is along the dimer axis, both the bright and dark dimer modes are excited [34], with peak wavelengths of 791.0 and 704.3 nm, respectively; (ii) when the electric dipole is in the middle of the dimer with $\boldsymbol{p}$ normal to the dimer axis, only the dark dimer mode can be excited with a stronger absorption at 704.3 nm, indicating a

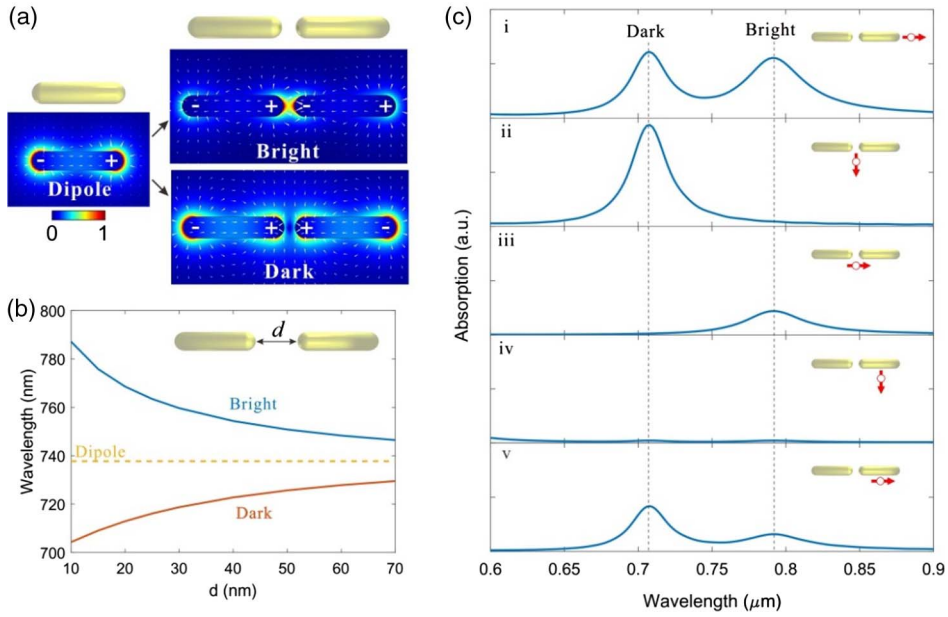

Fig. 1. Au nanorod dimer excitation with an electric dipole. (a) Mode profile and surface charge distribution of a longitudinal dipole mode in a single Au nanorod and hybridized bright and dark modes in a nanorod dimer; (b) resonant wavelengths of bright and dark modes as a function of dimer spacing d. The yellow dashed line denotes the resonant wavelength of a dipole mode in a single rod. The length and diameter of each nanorod are 95 and 20 nm, respectively. (c) Absorption spectra of the Au nanorod dimer under different electric dipole excitation conditions. The dimer spacing d is 10 nm. The electric dipole is located 20 nm away from the Au nanorod dimer. The red arrow indicates the electric dipole moment orientation and position relative to the nanorod dimer. The bright and dark modes are located at the wavelengths of 791.0 and 704.3 nm, respectively.

larger excitation efficiency of the dark mode; (iii) when the electric dipole oscillates parallel to the dimer axis in the middle of the dimer, only the bright dimer mode can be excited with a weaker absorption at 791.0 nm compared with case (i); (iv) when the electric dipole is offset to the middle of the right nanorod of the dimer and $\boldsymbol{p}$ is normal to the dimer axis, neither the bright nor dark mode is efficiently excited, as is shown by the small bumps at bright and dark resonances in the absorption spectrum; and (v) when the electric dipole is at the same position as case (iv) but oscillates parallel to the dimer axis, both bright and dark modes can be excited, but not as efficiently as in case (i).

The above-mentioned results can be explained by the coupling factor $\boldsymbol{p}\cdot\boldsymbol{E}$, where $\boldsymbol{E}$ is the electric field of the dimer mode. The mode with $\boldsymbol{E}$ perpendicular to $\boldsymbol{p}$ cannot be efficiently excited due to $\boldsymbol{p}\cdot\boldsymbol{E}=0$. This explains why only the dark (bright) mode can be excited in cases (ii) and (iii), and both modes cannot be efficiently excited in case (iv). Another factor to determine the excitation efficiency is the overlap between $\boldsymbol{E}$ and $\boldsymbol{p}$, which is the reason for a weaker excitation of bright and/or dark modes in cases (iii) and (v) compared with case (i).

For real cases, we replace the electric dipole with an Au nanorod, forming the plasmonic strong coupling system studied in this paper, as shown in Fig. 2(a). Thanks to the recently developed nanomanipulation techniques [4,35], this kind of strongly coupled nanorod structure can be experimentally realized with high precision. To efficiently excite the dark dimer mode, the Au nanorod is placed along the middle line perpendicular to the dark nanorod dimer axis. The plane wave polarized along the Au nanorod axis is normally incident on the structure from the top to excite the longitudinal dipole mode in the single nanorod, resembling case (ii) in Fig. 1(c), where only a dark dimer mode can be activated by the nanorod dipole. The separation between the dipolar nanorod and dimer h is defined as coupling distance in the following discussion, which is depicted in the inset of Fig. 2(a). Without loss of generality, we assume the whole structure is surrounded by air. To ensure the dipole and dark resonators have the same resonant frequency, the nanorod dimer has a rod length $L_d=95$ nm and dimer spacing $d=30$ nm. The single Au nanorod has a length $L_b=90.4$ nm. With such a parameter, the resonant wavelengths of the dimer dark mode and nanorod dipole mode are 722 nm, as depicted in Fig. 2(b). The linewidths of the dipole and dark dimer modes are $\gamma=2.05\times10^{13}$ Hz and $\kappa=1.67\times10^{13}$ Hz, respectively. As expected, the dark mode has a narrower linewidth than the dipole mode, i.e., a lower loss of the dark dimer mode.

Figure 3(a) shows the scattering spectra of the coupled nanorods with different separating distance h. The dashed curve is the scattering spectra of a single nanorod near dipole resonance. The single peaked resonance of an individual nanorod splits into two peaks when a dipolar nanorod is coupled to the dark dimer. As depicted in Fig. 3(b), the spectral splitting monotonically increases with h decreasing, where the associated coupling becomes stronger. For example, the splitting is 32.2 nm at $h=50$ nm and is increased to 94.7 nm at $h=10$ nm. The spectral splitting at $h=10$ nm corresponds to a frequency splitting of $\Omega=5.3\times10^{13}$ Hz (219.2 meV). Here, the relation between spectral splitting and the linewidths of the dipole and dark resonators fulfills the strong coupling condition $\Omega>\gamma+\kappa$ in the frequency domain [36]. The two peaks at $h=10$ nm locate at 686.2 and 780.9 nm, respectively, and the corresponding field profiles and charge distributions are shown in the inset of Fig. 3(a). At 686.2 nm, the surface charges at the nanorod end in the coupling region have the same sign, and the field intensity in the gap is relatively low, forming an antibonding-like hybridized resonance in the strongly coupled nanorods, while at 780.9 nm, field intensity is enhanced in the gap region, and the charges have the opposite signs for the dimer and the single rod in the coupling region, forming a bonding-like hybridized resonance. For the hybridized resonances, the nonzero dipole moments mainly located in the dipolar nanorod contribute to most of the radiative loss in the coherent energy exchange process.

Anticrossing behavior is another characteristic signature for strong coupling. Figure 4 shows the scattering spectra of the coupled nanorods with varying dipolar nanorod length (L_b). Other parameters are the same as in Fig. 3. The resonant wavelength in the dipole mode has a nearly linear dependence on nanorod length, as the red dashed line depicts in Fig. 4. The white dashed line shows the resonant wavelength of the dark dimer mode. With increasing L_b, the original single-peaked scattering spectrum gradually splits into two peaks near the crossing area of the white and red dashed lines. When further increasing L_b, the coupling effect decreases owing to larger

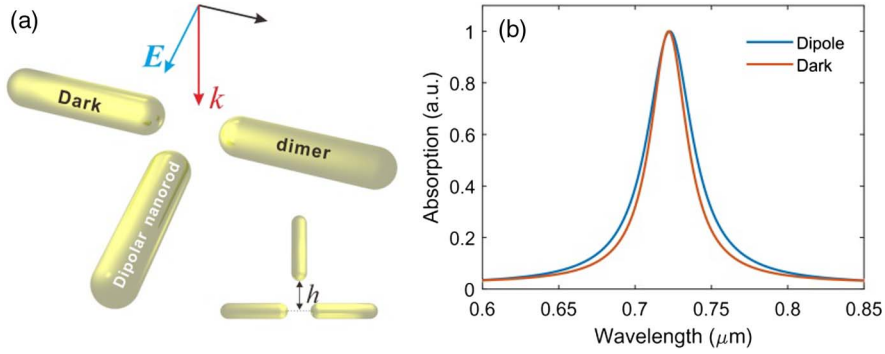

Fig. 2. (a) Schematic of plasmonic strong coupling in an Au nanorod structure. A single nanorod is placed along the middle line of the nanorod dimer with a separation of h, as denoted in the inset. A normally incident plane wave with a wave vector $\boldsymbol{k}$ is linearly polarized along the axis of a single nanorod. (b) Absorption spectra of the dipole mode in a single nanorod (blue) and dark mode in a nanorod dimer (red). The rod length and spacing of the dimer are 95 and 30 nm, respectively. The length of the single nanorod is 90.4 nm. The diameter of all nanorods is 20 nm.

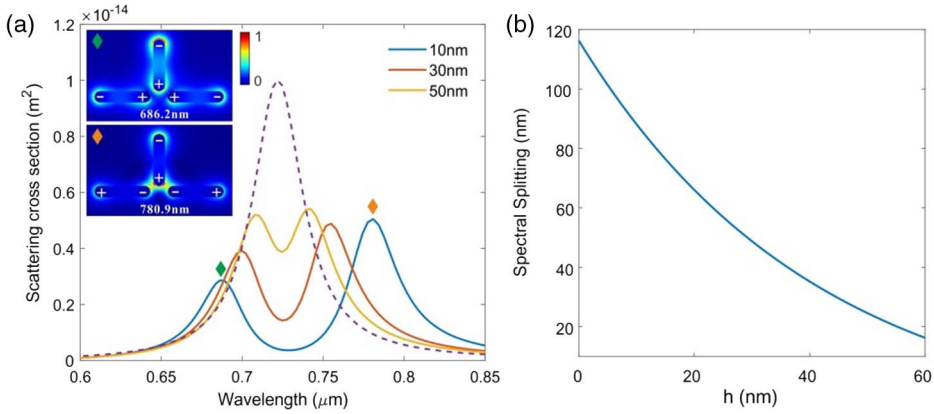

Fig. 3. (a) Scattering spectral splitting of the coupled nanorods with different coupling distance. The dashed curve shows the scattering of an individual dipolar nanorod. Electric field profiles of the coupled nanorods with a coupling distance $h = 10$ nm at 686.2 and 780.9 nm. Plus and minus signs denote the surface charge distribution. (b) The dependence of spectral splitting on the coupling distance h.

frequency detuning between the dimer and the single nanorod, and the scattering returns to a single peaked spectrum. Thus anticrossing behavior between the dipole and dark dimer modes is clearly shown in Fig. 4. It is worth mentioning that a larger L_b leads to a stronger scattering of the coupled nanorods, as the bright yellow color shows in Fig. 4.

To gain a deeper physical insight into the strong coupling process, we plot temporal electromagnetic energy (represented by the electric field) exchange between the dipole mode and the dark dimer mode in Fig. 5. The electric field is recorded by a time domain monitor set at 1 nm away from the nanorod end, as depicted in the inset of Fig. 5. Figure 5(a) shows the Rabi-like oscillation of energy exchange between the dipole and the dark dimer modes within the strong coupling regime, as the blue curves show in Fig. 3(a). The period of energy exchange is 19 fs, which equals the reciprocal of spectral splitting as Ω^{-1}. When the resonant frequency of the dipole mode is detuned from that of the dark dimer mode by changing L_b, for example, to 98 nm, the energy of the dipole mode is only partially

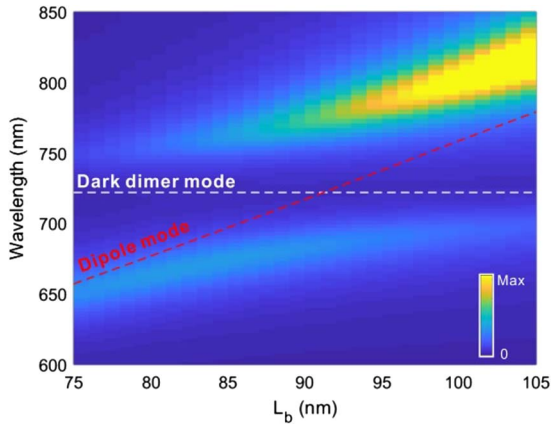

Fig. 4. Scattering spectra of the coupled nanorods with varying dipole resonator length L_b. The white and red dashed lines correspond to an unperturbed dark dimer mode and the dipole mode. The saturated scattering intensity on the upper-right corner is provided intentionally to get better contrast for the lower scattering branch due to a much larger scattering of the dipolar nanorod with longer L_b.

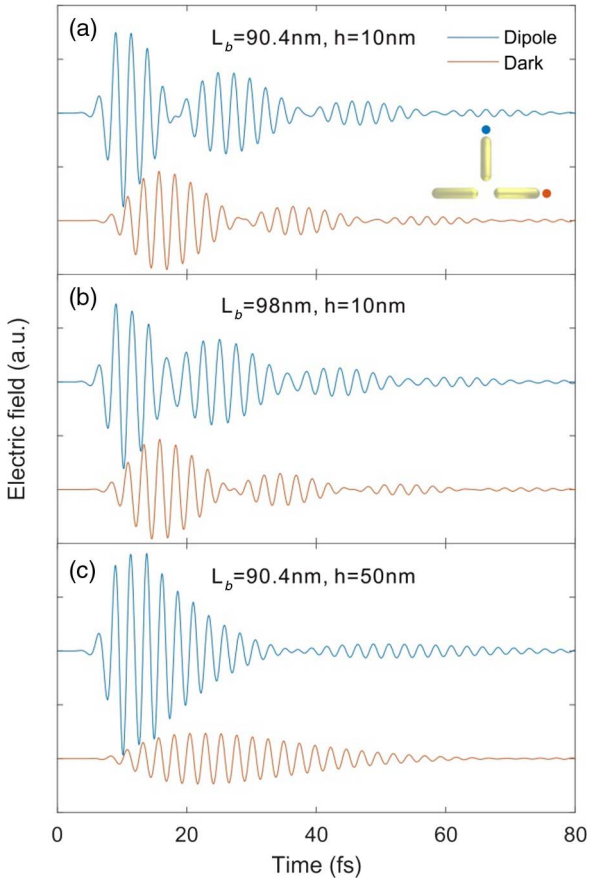

Fig. 5. Coherent energy exchange between the dipole mode and the dark dimer mode. (a) Complete energy exchange within the strong coupling regime, (b) partial energy exchange with a detuned frequency between the dipole and the dark dimer modes, (c) energy exchange with a lower exchange rate in the weakly coupled dipole and dark dimer modes. Time-dependent electric field amplitudes near the dipolar nanorod and the dark dimer are measured at the corresponding colored spots denoted in the inset of (a), which are 1 nm away from the rod end. The parameters of coupled nanorods are the same as in Fig. 3, except L_b and h.

transferred to the dark dimer mode, as depicted in Fig. 5(b), which is in stark contrast to the nearly complete energy transfer in the strong coupling case. Figure 5(c) plots the energy exchange at a lower coupling strength by increasing the coupling distance h to 50 nm. In this case, the time of the first period energy exchange is ~50 fs, and the damping rate of plasmon resonance exceeds the energy coupling rates, making it difficult for more energy exchange. Therefore, the resonant frequency matching and strong near-field interaction between the coupled dipole and dark dimer mode ensure efficient electromagnetic energy exchange, which is crucial for plasmonic strong coupling.

For the potential application of the proposal, first, we think it can be used as a highly compact approach to exciting and investigating dark modes in individual nanorod dimers with strong coupling. Second, as the spectral response is highly sensitive to material and environmental parameters [see, for example, Fig. 3(b)], it may be adapted for a plasmonic ruler or sensing down on the nanometer scale [37]. Third, the rapid coherent energy exchange of the strongly coupled structure could find promising applications in dark-mode-based plasmonic devices and ultrafast optical processes, which may also be intermediated via the nanorod dipole from the optical far field. Finally, the tunable splitting of double-peaked spectra in strongly coupled nanorods may also offer an opportunity for efficient nonlinear wave mixing with matched pump frequencies by tuning the coupling distance [38,39].

3. CONCLUSION

In summary, we studied plasmonic dark dimer mode excitation and its strong coupling with a nanorod dipole in Au nanorods. Selective excitation of bright and dark modes in a nanorod dimer can be achieved by a properly arranged electric dipole, which can be qualitatively determined by a coupling factor $\boldsymbol{p} \cdot \boldsymbol{E}$ related to the overlap of dipole moment $\boldsymbol{p}$ and plasmonic modal electric field $\boldsymbol{E}$. By replacing the dipole with an Au nanorod as a dipole antenna, the plane wave excited nanorod dipole could be efficiently coupled with the dark dimer mode with suppressed radiative loss. Near-field coupling of the nanorod dipole and dark dimer modes leads to spectral splitting of the original uncoupled single-peaked resonance, which increases with the decreasing coupling distance. The strong coupling criterion is fulfilled when the coupling distance is small enough (e.g., 10 nm). The characteristic anticrossing feature of strong coupling is revealed while changing the resonance frequency detuning of the strongly coupled modes. Rabi-like coherent electromagnetic energy exchange between dipole and dark modes occurs when plasmonic interaction enters the strong coupling regime. Our results provide an effective method to activate dark dimer modes through free-space radiation and coherently exchange plasmonic excitations at nanoscale, which may offer new opportunities for nanoplasmonic applications such as nanolasers or nanosensors. The proposed low-cost colloidal nanorod-based structures are also promising for further integration with quantum emitters to realize future quantum devices [40].

Funding. National Natural Science Foundation of China (NSFC) (11527901, 61475136, 61635009); Fundamental Research Funds for the Central Universities; China Postdoctoral Science Foundation (2018M632454, BX201700207).

REFERENCES

1. W. L. Barnes, A. Dereux, and T. W. Ebbesen, "Surface plasmon subwavelength optics," Nature **424**, 824–830 (2003).
2. Z. Wang, X. Meng, A. V. Kildishev, A. Boltasseva, and V. M. Shalaev, "Nanolasers enabled by metallic nanoparticles: from spasers to random lasers," Laser Photon. Rev. **11**, 1700212 (2017).
3. J. N. Anker, W. P. Hall, O. Lyandres, N. C. Shah, J. Zhao, and R. P. Van Duyne, "Biosensing with plasmonic nanosensors," Nat. Mater. **7**, 442–453 (2008).
4. H. Shen, R. Y. Chou, Y. Y. Hui, Y. He, Y. Cheng, H.-C. Chang, L. Tong, Q. Gong, and G. Lu, "Directional fluorescence emission from a compact plasmonic-diamond hybrid nanostructure," Laser Photon. Rev. **10**, 647–655 (2016).
5. R. Chikkaraddy, B. de Nijs, F. Benz, S. J. Barrow, O. A. Scherman, E. Rosta, A. Demetriadou, P. Fox, O. Hess, and J. J. Baumberg, "Single-molecule strong coupling at room temperature in plasmonic nanocavities," Nature **535**, 127–130 (2016).
6. H. Wang, D. W. Brandl, P. Nordlander, and N. J. Halas, "Plasmonic nanostructures: artificial molecules," Acc. Chem. Res. **40**, 53–62 (2007).
7. N. Papasimakis, V. A. Fedotov, N. I. Zheludev, and S. L. Prosvirnin, "Metamaterial analog of electromagnetically induced transparency," Phys. Rev. Lett. **101**, 253903 (2008).
8. R. Guo, M. Decker, F. Setzpfandt, I. Staude, D. N. Neshev, and Y. S. Kivshar, "Plasmonic Fano nanoantennas for on-chip separation of wavelength-encoded optical signals," Nano Lett. **15**, 3324–3328 (2015).
9. C. Wu, A. B. Khanikaev, R. Adato, N. Arju, A. A. Yanik, H. Altug, and G. Shvets, "Fano-resonant asymmetric metamaterials for ultrasensitive spectroscopy and identification of molecular monolayers," Nat. Mater. **11**, 69–75 (2011).
10. P. Nordlander, C. Oubre, E. Prodan, K. Li, and M. I. Stockman, "Plasmon hybridization in nanoparticle dimers," Nano Lett. **4**, 899–903 (2004).
11. H. Xu, J. Aizpurua, M. Käll, and P. Apell, "Electromagnetic contributions to single-molecule sensitivity in surface-enhanced Raman scattering," Phys. Rev. E **62**, 4318–4324 (2000).
12. H. Aouani, M. Rahmani, M. Navarro-Cia, and S. A. Maier, "Third-harmonic-upconversion enhancement from a single semiconductor nanoparticle coupled to a plasmonic antenna," Nat. Nanotechnol. **9**, 290–294 (2014).
13. A. F. Koenderink, "Single-photon nanoantennas," ACS Photon. **4**, 710–722 (2017).
14. A. M. Michaels, J. Jiang, and L. Brus, "Ag nanocrystal junctions as the site for surface-enhanced Raman scattering of single rhodamine 6G molecules," J. Phys. Chem. B **104**, 11965–11971 (2000).
15. K. D. Osberg, N. Harris, T. Ozel, J. C. Ku, G. C. Schatz, and C. A. Mirkin, "Systematic study of antibonding modes in gold nanorod dimers and trimers," Nano Lett. **14**, 6949–6954 (2014).
16. S. Zhang, L. Chen, Y. Huang, and H. Xu, "Reduced linewidth multipolar plasmon resonances in metal nanorods and related applications," Nanoscale **5**, 6985–6991 (2013).
17. D. E. Gomez, Z. Q. Teo, M. Altissimo, T. J. Davis, S. Earl, and A. Roberts, "The dark side of plasmonics," Nano Lett. **13**, 3722–3728 (2013).
18. M. Ramezani, A. Halpin, A. I. Fernández-Domínguez, J. Feist, S. R.-K. Rodriguez, F. J. Garcia-Vidal, and J. Gómez Rivas, "Plasmon-exciton-polariton lasing," Optica **4**, 31–37 (2017).
19. T. K. Hakala, H. T. Rekola, A. I. Vakevainen, J. P. Martikainen, M. Necada, A. J. Moilanen, and P. Torma, "Lasing in dark and bright modes of a finite-sized plasmonic lattice," Nat. Commun. **8**, 13687 (2017).
20. D. Zheng, S. Zhang, Q. Deng, M. Kang, P. Nordlander, and H. Xu, "Manipulating coherent plasmon-exciton interaction in a single silver nanorod on monolayer WSe_2," Nano Lett. **17**, 3809–3814 (2017).

21. B. Yun, G. Hu, J. Cong, and Y. Cui, "Fano resonances induced by strong interactions between dipole and multipole plasmons in T-shaped nanorod dimer," Plasmonics **9**, 691–698 (2014).
22. Z. J. Yang, Z. S. Zhang, L. H. Zhang, Q. Q. Li, Z. H. Hao, and Q. Q. Wang, "Fano resonances in dipole-quadrupole plasmon coupling nanorod dimers," Opt. Lett. **36**, 1542–1544 (2011).
23. P. K. Jha, M. Mrejen, J. Kim, C. Wu, X. Yin, Y. Wang, and X. Zhang, "Interacting dark resonances with plasmonic meta-molecules," Appl. Phys. Lett. **105**, 111109 (2014).
24. N. Liu, L. Langguth, T. Weiss, J. Kastel, M. Fleischhauer, T. Pfau, and H. Giessen, "Plasmonic analogue of electromagnetically induced transparency at the Drude damping limit," Nat. Mater. **8**, 758–762 (2009).
25. Z. J. Yang, Z. H. Hao, H. Q. Lin, and Q. Q. Wang, "Plasmonic Fano resonances in metallic nanorod complexes," Nanoscale **6**, 4985–4997 (2014).
26. C. J. Tang, P. Zhan, Z. S. Cao, J. Pan, Z. Chen, and Z. L. Wang, "Magnetic field enhancement at optical frequencies through diffraction coupling of magnetic plasmon resonances in metamaterials," Phys. Rev. B **83**, 041402 (2011).
27. R. Ameling and H. Giessen, "Cavity plasmonics: large normal mode splitting of electric and magnetic particle plasmons induced by a photonic microcavity," Nano Lett. **10**, 4394–4398 (2010).
28. Z. Xi, Y. Lu, W. Yu, P. Yao, P. Wang, and H. Ming, "Strong coupling between plasmonic Fabry–Pérot cavity mode and magnetic plasmon," Opt. Lett. **38**, 1591–1593 (2013).
29. R. Ameling, D. Dregely, and H. Giessen, "Strong coupling of localized and surface plasmons to microcavity modes," Opt. Lett. **36**, 2218–2220 (2011).
30. P. Wang, Y. Wang, Z. Yang, X. Guo, X. Lin, X. C. Yu, Y. F. Xiao, W. Fang, L. Zhang, G. Lu, Q. Gong, and L. Tong, "Single-band 2-nm-line-width plasmon resonance in a strongly coupled Au nanorod," Nano Lett. **15**, 7581–7586 (2015).
31. D. Y. Lu, H. Liu, T. Li, S. M. Wang, F. M. Wang, S. N. Zhu, and X. Zhang, "Creation of a magnetic plasmon polariton through strong coupling between an artificial magnetic atom and the defect state in a defective multilayer microcavity," Phys. Rev. B **77**, 214302 (2008).
32. H. Chen, L. Shao, Q. Li, and J. Wang, "Gold nanorods and their plasmonic properties," Chem. Soc. Rev. **42**, 2679–2724 (2013).
33. P. B. Johnson and R. W. Christy, "Optical constants of the noble metals," Phys. Rev. B **6**, 4370–4379 (1972).
34. M. Liu, T. W. Lee, S. K. Gray, P. Guyot-Sionnest, and M. Pelton, "Excitation of dark plasmons in metal nanoparticles by a localized emitter," Phys. Rev. Lett. **102**, 107401 (2009).
35. S. C. Yang, H. Kobori, C. L. He, M. H. Lin, H. Y. Chen, C. Li, M. Kanehara, T. Teranishi, and S. Gwo, "Plasmon hybridization in individual gold nanocrystal dimers: direct observation of bright and dark modes," Nano Lett. **10**, 632–637 (2010).
36. D. G. Baranov, M. Wersäll, J. Cuadra, T. J. Antosiewicz, and T. Shegai, "Novel nanostructures and materials for strong light-matter interactions," ACS Photon. **5**, 24–42 (2017).
37. W. Chen, S. Zhang, Q. Deng, and H. Xu, "Probing of sub-picometer vertical differential resolutions using cavity plasmons," Nat. Commun. **9**, 801 (2018).
38. H. Harutyunyan, G. Volpe, R. Quidant, and L. Novotny, "Enhancing the nonlinear optical response using multifrequency gold-nanowire antennas," Phys. Rev. Lett. **108**, 217403 (2012).
39. M. Celebrano, X. Wu, M. Baselli, S. Grossmann, P. Biagioni, A. Locatelli, C. De Angelis, G. Cerullo, R. Osellame, B. Hecht, L. Duo, F. Ciccacci, and M. Finazzi, "Mode matching in multiresonant plasmonic nanoantennas for enhanced second harmonic generation," Nat. Nanotechnol. **10**, 412–417 (2015).
40. A. V. Akimov, A. Mukherjee, C. L. Yu, D. E. Chang, A. S. Zibrov, P. R. Hemmer, H. Park, and M. D. Lukin, "Generation of single optical plasmons in metallic nanowires coupled to quantum dots," Nature **450**, 402–406 (2007).